Cell

The Ubiquitin Binding Domain ZnF UBP Recognizes the C-Terminal Diglycine Motif of Unanchored Ubiquitin

Francisca E. Reyes-Turcu,[1] John R. Horton,[1] James E. Mullally,[1] Annie Heroux,[2] Xiaodong Cheng,[1] and Keith D. Wilkinson[1,*]
[1] Department of Biochemistry, Emory University School of Medicine, Atlanta, GA 30322, USA
[2] Department of Biology, Brookhaven National Laboratory, Upton, NY 11794, USA
*Contact: genekdw@emory.edu
DOI 10.1016/j.cell.2006.02.038

SUMMARY

Ubiquitin binding proteins regulate the stability, function, and/or localization of ubiquitinated proteins. Here we report the crystal structures of the zinc-finger ubiquitin binding domain (ZnF UBP) from the deubiquitinating enzyme isopeptidase T (IsoT, or USP5) alone and in complex with ubiquitin. Unlike other ubiquitin binding domains, this domain contains a deep binding pocket where the C-terminal diglycine motif of ubiquitin is inserted, thus explaining the specificity of IsoT for an unmodified C terminus on the proximal subunit of polyubiquitin. Mutations in the domain demonstrate that it is required for optimal catalytic activation of IsoT. This domain is present in several other protein families, and the ZnF UBP domain from an E3 ligase also requires the C terminus of ubiquitin for binding. These data suggest that binding the ubiquitin C terminus may be necessary for the function of other proteins.

INTRODUCTION

Ubiquitin is a highly conserved 76 residue protein whose conjugation to substrate proteins acts as a signal to alter protein localization or function and/or to regulate protein-protein interactions (Hershko and Ciechanover, 1998; Hicke, 2001; Pickart, 2004; Sun and Chen, 2004). Ubiquitin is conjugated to target proteins via an isopeptide bond formed between its C-terminal residue (G76) and a side-chain lysine on the target protein. Conjugation of a single ubiquitin to target proteins is required for diverse processes such as receptor-mediated signaling, endocytosis, viral budding, and maintenance of chromatin (Sigismund et al., 2004). Additionally, any of seven ubiquitin lysines can be utilized to form an isopeptide bond to another ubiquitin (Pickart and Fushman, 2004), resulting in polyubiquitin chains having different conformations (Varadan et al., 2004). One of the best understood functions of polyubiquitin is to direct proteins to the proteasome to be degraded (Welchman et al., 2005). The canonical degradation signal is composed of four or more ubiquitins linked through K48 on ubiquitin. Linkage of polyubiquitin through other lysines appears to target proteins for nondegradative fates. Polyubiquitin chains have polarity: The proximal end is defined as the end proximal to the target protein to which it is conjugated (or, in unanchored chains, the end that contains a free C terminus), while the distal end is the end farthest from the conjugated substrate.

A number of ubiquitin binding domains have been described, and, in some cases, the molecular details of the interactions are known (Alam et al., 2004; Davies et al., 2003; Hicke et al., 2005; Mueller et al., 2004; Ohno et al., 2005; Prag et al., 2003, 2005; Sundquist et al., 2004; Swanson et al., 2003). Most of these proteins contact the hydrophobic face of ubiquitin, centered on I44; however, recently, two new ubiquitin binding domains were reported to contact ubiquitin through surfaces that are not centered on I44 (Bienko et al., 2005; Lee et al., 2006; Penengo et al., 2006 [this issue of *Cell*]).

The recognition of ubiquitin by deubiquitinating enzymes (DUBs) provides a model for understanding the binding of other ubiquitin binding proteins. DUBs are proteases that hydrolyze the isopeptide bond between ubiquitin and target proteins (Amerik and Hochstrasser, 2004; Wilkinson, 1997) and between adjacent ubiquitins in polyubiquitin chains, thereby recycling free ubiquitin (Amerik et al., 1997; Doelling et al., 2001; Lindsey et al., 1998). The disassembly of polyubiquitin chains is necessary to avoid their accumulation, which can inhibit the proteasome (Amerik et al., 1997; Lam et al., 2000). Human isopeptidase T (IsoT or USP5) is a homolog of *S. cerevisiae* UBP14, which is responsible for the disassembly of the majority of unanchored polyubiquitin chains (Amerik et al., 1997). IsoT nonprocessively disassembles unanchored chains, releasing one ubiquitin at a time from the proximal end of the chain. Modification of the proximal ubiquitin's C terminus by esterification or removal of G76 markedly reduces the rate of cleavage by IsoT (Wilkinson et al., 1995).

IsoT-mediated hydrolysis of ubiquitin amidomethyl coumarin (Ub-AMC) is stimulated by low concentrations of free monoubiquitin with an unmodified C terminus, suggesting the presence of an activation domain in IsoT (Dang et al., 1998). The requirement for an unmodified C terminus in monoubiquitin to activate Ub-AMC hydrolysis and the requirement for an unmodified C terminus to achieve efficient hydrolysis of unanchored polyubiquitin chains (Wilkinson et al., 1995) suggest that the activation domain is the site that interacts with the proximal ubiquitin in polyubiquitin chains.

Figure 1A depicts the four putative ubiquitin binding domains of IsoT: the UBP (ubiquitin-specific processing protease) catalytic domain formed by noncontiguous regions containing the active-site Cys and His box (Amerik et al., 1997), two ubiquitin-associated (UBA) domains, and a zinc-finger ubiquitin binding domain (ZnF UBP). The latter domain is also known as the *p*olyubiquitin-*a*ssociated *z*inc finger (PAZ) domain (Hook et al., 2002; Seigneurin-Berny et al., 2001). The prevailing model is that, together, these domains coordinate the binding and hydrolysis of polyubiquitin chains; at least one domain comprises the S1′ site and binds the proximal ubiquitin, thus activating hydrolysis at the active site (Figure 1B). The others form the S1–S3 sites and bind the distal ubiquitins on the chain (Wilkinson et al., 1995). For Ub-AMC hydrolysis, the ubiquitin moiety of Ub-AMC binds to the S1 (catalytic) site, and free monoubiquitin binds the activation or S1′ site (Figure 1C). In both assays, occupancy of the S1′ site by ubiquitin bearing a free C terminus is thought to be necessary for optimal activity.

Here we show structurally and biochemically that the ZnF UBP domain of IsoT is the S1′ site and, as such, is responsible for recognizing the diglycine motif on the C terminus of unanchored polyubiquitin chains. The ZnF UBP domain is present in several conserved protein families: deubiquitinating enzymes such as mammalian USP3, USP5, USP13, USP44, USP45, USP49, and USP51 and *S. cerevisiae* UBP8; a RING E3 ligase (known as IMP, *i*mpedes *m*itogenic signal *p*rogression, or BRAP2, *BR*CA1-*a*ssociated *p*rotein *2*); and HDAC6, a microtubule deacetylase (Amerik et al., 2000; Ingvarsdottir et al., 2005; Li et al., 1998; Matheny et al., 2004; Quesada et al., 2004; Seigneurin-Berny et al., 2001). We find that the ZnF UBP domain of the *S. cerevisiae* homolog of human IMP (scIMP, or YHL010c) binds ubiquitin and requires the C-terminal glycine of ubiquitin for binding, suggesting that this novel mode of binding is conserved among ZnF UBP domains. The present study represents the structural and biochemical characterization of a ZnF UBP domain and has important implications for understanding the function of other proteins containing this domain.

RESULTS

The Activation Domain, S1′ Site, of IsoT Binds Monoubiquitin Tightly

To quantitate the binding of monoubiquitin to IsoT, we developed a binding assay utilizing fluorescence anisotropy measurements. The fluorescent probe (IA-Ub) consists of a K48C mutant monoubiquitin labeled with a thiol-reactive fluorescent dye (see Experimental Procedures). IsoT binds IA-Ub, and this binding can be competed by monoubiquitin but not Ub^{1-75}, a mutant ubiquitin lacking the C-terminal glycine (Figures 1D and 1E, respectively). The competitive binding suggests that IA-Ub and monoubiquitin bind to the same site on IsoT with similar binding constants—75 ± 2 nM and 72 ± 9 nM, respectively—and that this binding requires an unmodified C terminus. In the context of binding to unanchored polyubiquitin chains, these data suggest that this monoubiquitin binding domain forms the S1′ pocket responsible for recognizing the presence of an unmodified free C terminus.

The Activation Domain, S1′ Site, of IsoT Is the ZnF UBP Domain

To identify the domain of IsoT that requires an unmodified ubiquitin C terminus for binding, we performed tryptic proteolysis on the purified, recombinant full-length IsoT and identified a 15 kDa fragment capable of binding to an affinity column containing wild-type monoubiquitin but not to a column containing G76C monoubiquitin (see Figure S1A in the Supplemental Data available with this article online). Using mass spectrometry and N-terminal sequencing, we determined that the isolated 15 kDa fragment is comprised of amino acids 163–291, corresponding to the ZnF UBP domain of IsoT. The recombinant IsoT ZnF UBP domain retains the property of binding to an unmodified ubiquitin C terminus (Figure S1B). We measured the binding affinity between the ZnF UBP domain and ubiquitin by isothermal titration calorimetry (ITC). The domain bound a single molecule of ubiquitin (K_D = 2.82 ± 0.09 μM, $\Delta H_{apparent}$ = −20.9 ± 0.3 kcal/mol, and $\Delta S_{apparent}$ = −44 ± 1 cal/mol/deg) (Figure 1F). This binding is tighter than that of most other isolated ubiquitin binding domains (10–500 μM) (Hicke et al., 2005). However, the binding is ~30-fold weaker than that of full-length IsoT, suggesting that the region (or regions) outside of the ZnF UBP domain also contributes to the binding affinity for monoubiquitin.

Structure of the IsoT ZnF UBP Domain

We crystallized the ZnF UBP domain of IsoT and determined its structure to a resolution of 2.09 Å (Table S1). The domain crystallizes as a disulfide-linked dimer (see Discussion), but, as both molecules in the unit cell are identical, we will discuss only the monomeric structure. The ZnF UBP domain mainly consists of five antiparallel β strands (2↑ 1↓ 3↑ 4↓ 5↑), with a topological switch between strands β1 and β3, and two α helices, with helix αA on one side of strands β1 and β2 and helix αB on the other side of strands β3 to β5 (Figures 2A–2B). The domain adopts a compact fold with a deep pocket formed predominantly by residues of strands β1 and β4 and loop L2A; Y261 lies in the bottom of the pocket, while W209, Y259, and the guanidine group of R221 line the sides of pocket (Figures 2C). One zinc ion is chelated tetrahedrally

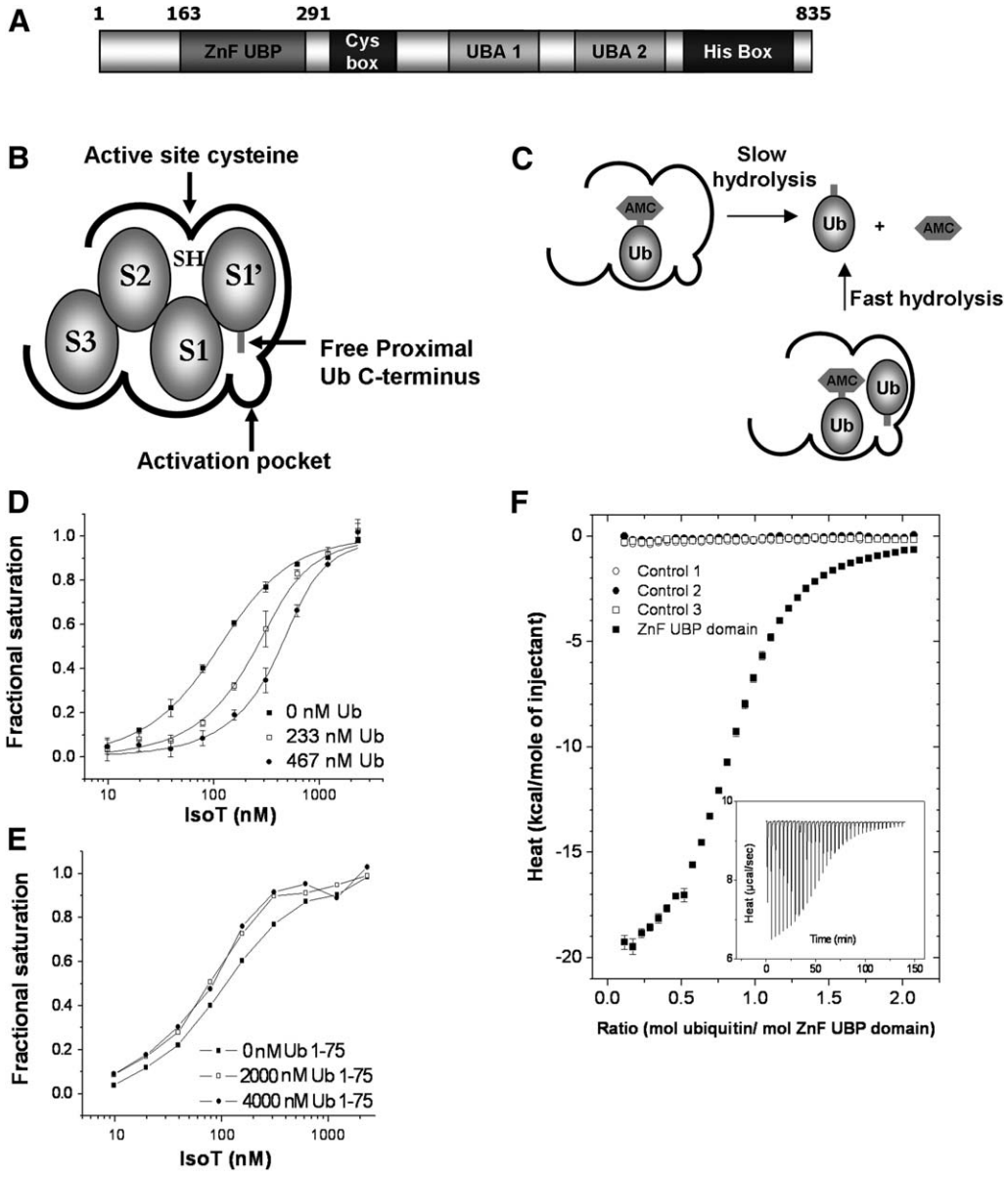

Figure 1. The C Terminus of Ubiquitin Is Required for Binding to the Activation Domain of IsoT

(A) IsoT ubiquitin binding domains. The UBP domain consists of the Cys and His box depicted in black.

(B) Putative binding of K48-linked tetraubiquitin to IsoT. The proximal ubiquitin (Ub) occupies the activation or S1′site, and the distal ubiquitins occupy the S1, S2, and S3 sites.

(C) Model of the enzymatic mechanism of IsoT using Ub-AMC as a substrate. Ub-AMC binds to the S1 or active site, and it is hydrolyzed to ubiquitin and AMC. Free ubiquitin binds the S1′site of IsoT, stimulating the hydrolysis of Ub-AMC at the S1 site.

(D) Competitive binding of IA-Ub and Ub to IsoT. IA-Ub concentration was 80 nM for all binding assays. Ub concentration was increased from 0 to 467 nM. The K_D measured for IA-Ub is 75 ± 2 nM, while the K_D for ubiquitin (Ub) is 72 ± 9 nM. Error bars delineate the standard deviation of three measurements.

(E) Ub^{1-75}does not compete with IA-Ub for binding to IsoT. IA-Ub concentration was 80 nM for all binding assays. Ub^{1-75} was increased from 0 to 4000 nM.

(F) Binding of IsoT ZnF UBP domain to ubiquitin as measured by ITC. Ubiquitin (1362 μM) was injected into 1.4 ml of buffer containing the ZnF UBP domain of IsoT (50 μM) in 35 injections of 3 μl each. Controls 1, 2, and 3 consist of injecting buffer into buffer, ubiquitin into buffer, or buffer into the ZnF UBP domain of IsoT, respectively. The inset shows one representative titration of the ZnF UBP domain with ubiquitin. Error bars delineate the standard deviation of three measurements.

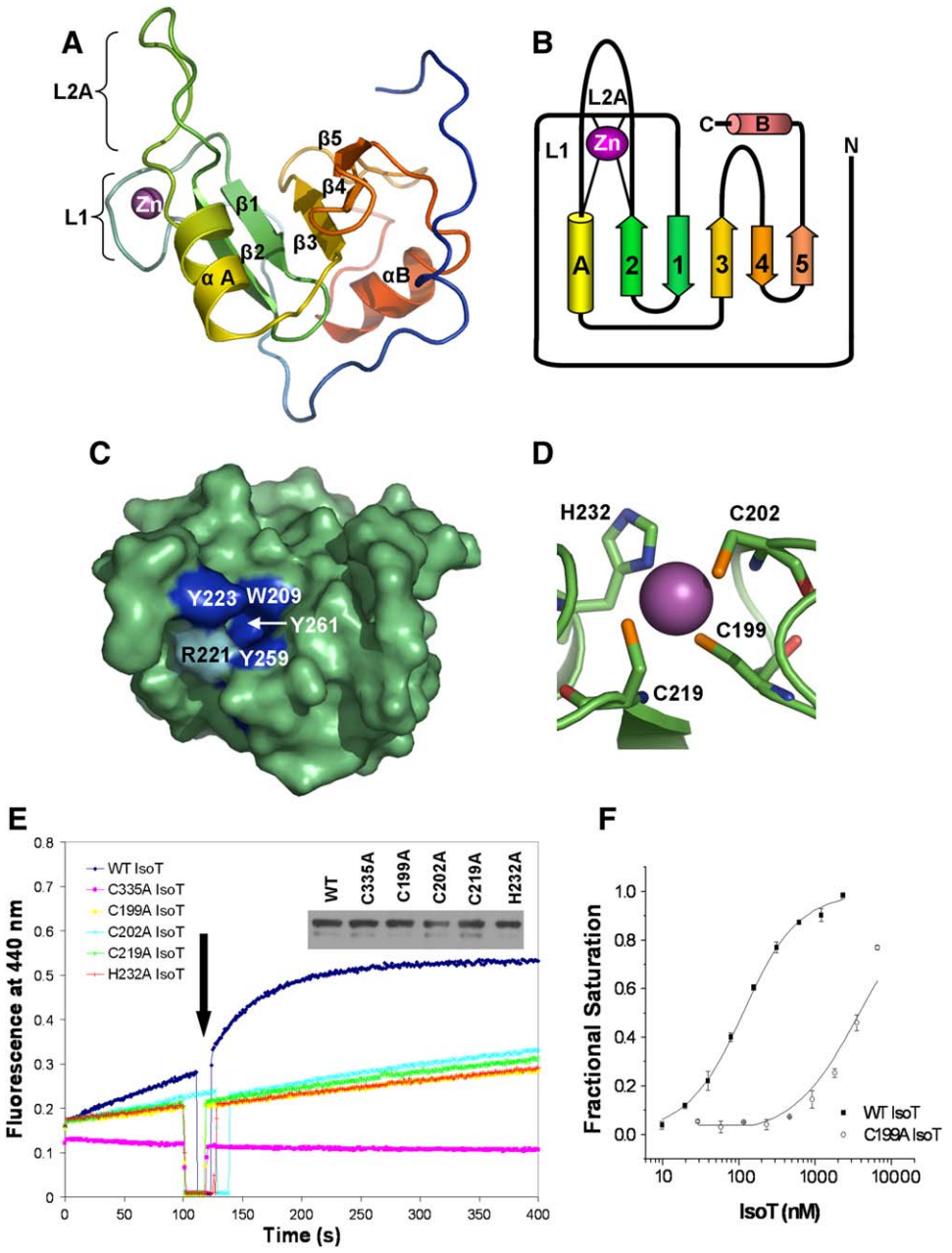

Figure 2. The ZnF UBP Domain of IsoT

(A) Ribbon diagram of the crystal structure of the IsoT ZnF UBP domain alone.

(B) Topology of the unliganded IsoT ZnF UBP domain.

(C) Surface representation of the deep hydrophobic pocket of IsoT. The ZnF UBP domain is shown in green, the aromatic residues that form the hydrophobic pocket are colored in blue, and R221 is colored in cyan.

(D) Residues that bind to zinc. The Zn is represented as a sphere colored magenta. Residues that chelate the metal are shown as sticks colored as follows: green, carbons; dark blue, nitrogens; orange, sulfurs.

(E) Submicromolar amounts of Ub do not activate the hydrolysis of Ub-AMC in ZnF UBP mutant IsoT. *E. coli* cell lysates (10 ng/μl) expressing wild-type (WT) IsoT or ZnF UBP domain mutant IsoT were incubated with 20 nM Ub-AMC. After ~100 s, 85 nM Ub was added to the reaction mixture (black arrow). The activity of the active-site point mutant, C335A IsoT, was determined to rule out any residual activity due to proteases/esterases present in the *E. coli* cell lysate. A Western blot of *E. coli* cell lysate expressing wild-type or mutant IsoT shows that similar amounts of IsoT point mutants were expressed (10 μg of cell lysate per lane).

(F) C199A IsoT shows a 50-fold decrease in affinity for IA-Ub compared to WT IsoT. IsoT binds IA-Ub with a K_D of 75 ± 2 nM, while C199A IsoT binds with a K_D of ≥3700 nM. Error bars delineate the standard deviation of three measurements.

by three cysteines (C199, C202, and C219) and one histidine (H232) (Figure 2D). C199 and C202 are located on loop L1, N-terminal to strand β1, while C219 and H232 are the last and first residues of strand β2 and helix αA, respectively.

We individually mutated the four Zn binding residues to alanine in full-length IsoT. Like wild-type IsoT, the mutant proteins are able to hydrolyze Ub-AMC, albeit at a slightly slower rate (Figure 2E, first 100 s of the time course). However, unlike wild-type IsoT, none of the point mutants were activated by the addition of free monoubiquitin (Figure 2E, 100 to 400 s of the time course). We purified one mutant (C199A) using a ubiquitin affinity column and showed that it exhibited decreased zinc binding (data not shown) and a ~50-fold decrease in binding affinity for IA-Ub (Figure 2F). Overall, this point mutant is correctly folded since over 89% of C199A IsoT can react with the active-site irreversible inhibitor ubiquitin vinyl sulfone (Ub-VS) (Figure S1C). The mutagenesis data indicate an important structural role for the zinc atom, perhaps as a stabilizing force for the interaction of two long loops: loop L1 and loop L2A between strand β2 and helix αA.

Structure of the IsoT ZnF UBP Domain in Complex with Ubiquitin

To define the nature of ubiquitin binding by the ZnF UBP domain, we crystallized this domain of IsoT in complex with ubiquitin (Table S2). The ZnF UBP domain/ubiquitin complex also crystallized as a disulfide-linked dimer, but, unlike the unliganded domain, it dimerized by domain swapping involving the N-terminal residues 173–196 (see Discussion). Confirming our biochemical data, the ZnF UBP domain primarily contacts the C terminus of ubiquitin (residues L71 through G76) (Figure 3A). These C-terminal residues form a rigid tail extending from the globular body of ubiquitin, penetrating deeply into the hydrophobic pocket of the ZnF UBP domain. The 12 residue loop L2A protrudes from the body of the ZnF UBP domain, interacting in an antiparallel fashion with the penetrating ubiquitin C terminus. The tip of the loop (F224) contacts the globular surface of ubiquitin (Figure 3B), forming hydrophobic interactions with two aliphatic side chains (L8 and I36) of ubiquitin. A total of approximately 500 $Å^2$ of surface area is occluded on each molecule upon formation of this complex. Notably, unlike many ubiquitin binding domains characterized, including UBA domains, I44 of ubiquitin does not contact the ZnF UBP domain. Furthermore, neither the ZnF UBP domain nor the full-length IsoT appears to require this residue for binding monoubiquitin (data not shown and Figure S1D).

The interactions with the C terminus of ubiquitin include an extensive network of direct and water-mediated hydrogen bonds and van der Waals contacts (Figures 4A–4E). The carboxyl oxygen atoms of ubiquitin G76 form two direct hydrogen bonds with the amide group of R221 and the hydroxyl group of Y261, respectively (Figure 4B). In addition, each carboxyl oxygen atom interacts with one water molecule, w1 or w2, respectively. Water molecule w1 is trapped in the bottom of the pocket, forming two additional hydrogen bonds with the backbone carbonyl oxygen of C219, which is one of the zinc ligands, and backbone amide of V234, which is 2 residues away from another zinc ligand, H232. Thus, the ubiquitin G76 binding site is directly linked to the metal center, with a distance of 7.5 Å between the zinc and the w1 water (Figure 4A). Water molecule w2 mediates a network of interactions involving (1) the ubiquitin R74 main-chain carbonyl group and amide group interacting with Y223 and (2) another water molecule, w3, interacting with the main-chain carbonyl group of R221 (Figure 4C). The backbone amide of ubiquitin G76 points to the face of the indole ring of W209, forming an N-H$\cdots\pi$ electron interaction (Figure 4D). The α carbon of ubiquitin G76 is within van der Waals contacts with the aromatic rings of Y259, Y261, and W209 (Figure 4A). Consistent with defects in hydrolysis seen with C-terminally modified polyubiquitin chains (Wilkinson et al., 1995), modeling of the G76A mutation of ubiquitin suggests that the β carbon of alanine would sterically clash with the aromatic rings of Y259 and Y261 (data not shown), generating strong repulsive interactions among the three residues.

The main-chain carbonyl oxygen of ubiquitin G75 forms two hydrogen bonds with the guanidino group of R221 (Figure 4D); notably, the positively charged R221 side chain does not interact directly with the carboxylate of ubiquitin G76. The peptide plane of G75-G76 is in parallel with the aromatic ring of Y259, whose side-chain hydroxyl group interacts with D264 (Figure 4E). The negatively charged side chain of D264 bridges between two arginines (R72 and R74) of ubiquitin (Figure 4E). The aromatic ring of Y223 from loop L2A packs together with L71 and L73 of ubiquitin (Figure 4E).

Residues that Contact the Diglycine Motif of Ubiquitin Are Required for Catalytic Activation of IsoT

We individually mutated the residues contacting ubiquitin in the ZnF UBP domain to test their contribution to the activation of IsoT. These residues are highly conserved among other ZnF UBP domains (Figure 4F). Seven point mutants were created, all of which were correctly folded since over 80% of each point mutant could react with the active-site-directed irreversible inhibitor Ub-VS (Figure S1C). All seven point mutants could hydrolyze Ub-AMC (Figure 5A and Figures S2A–S2B); however, three of these mutants (W209A, R221A, and Y261A) were not activated upon addition of free ubiquitin. These three residues are in close contact with the diglycine motif of ubiquitin, suggesting that recognition of diglycine is necessary for activation of IsoT. In contrast, the remaining four point mutants, Y223A, F224A, Y261A, and D264A, were activated upon addition of free ubiquitin, suggesting that contact with residues L8, I36, and L71-R74 of ubiquitin may not be essential for activation of IsoT.

Although ubiquitin activates Ub-AMC hydrolysis, it does not activate tetraubiquitin-chain disassembly (Figures S2C–S2D), suggesting that ubiquitin and the proximal

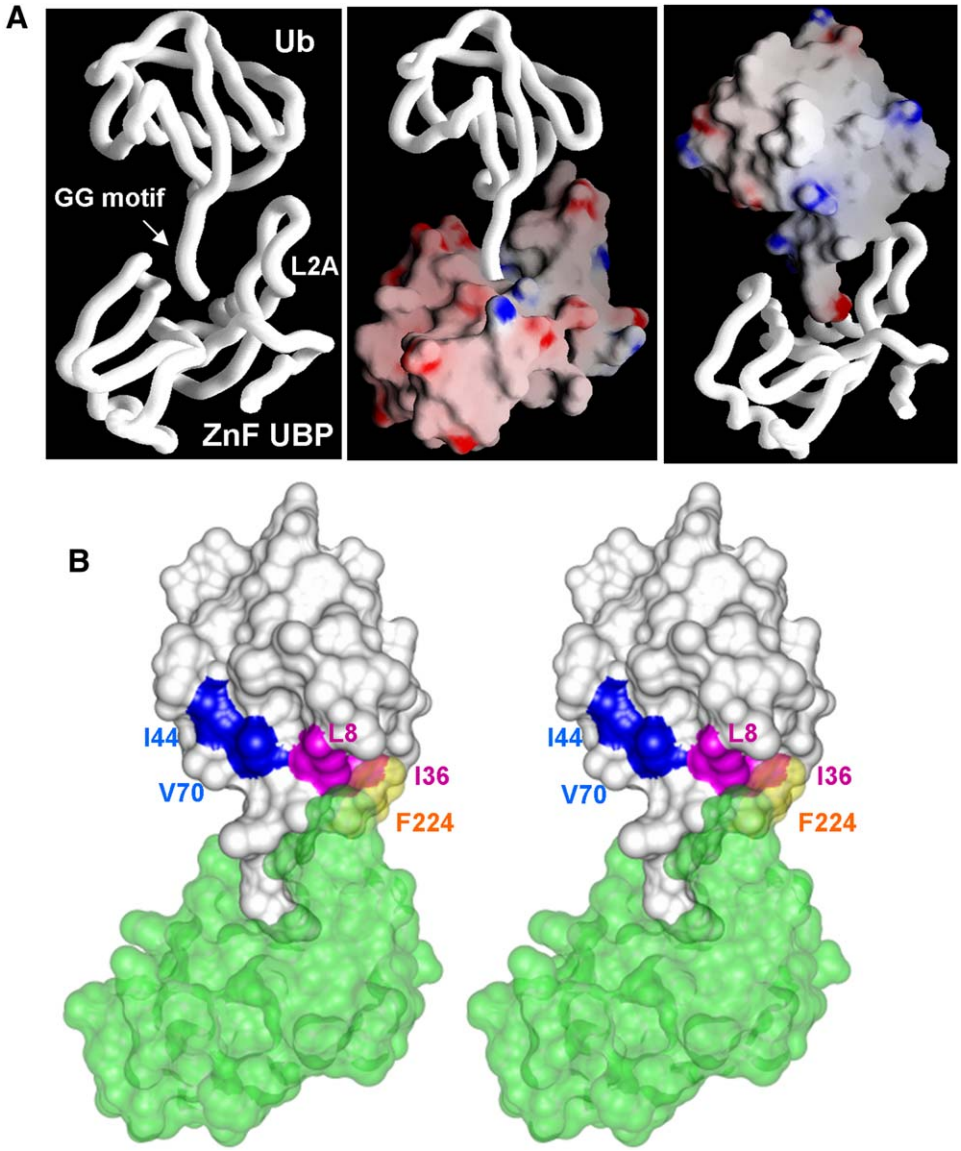

Figure 3. Structure of IsoT ZnF UBP Domain Bound to Ubiquitin

(A) Ribbon diagram and/or surface representation of the IsoT ZnF UBP domain bound to ubiquitin. Positive charges are represented in blue, negative charges are shown in red, and neutral residues are shown in white.

(B) Stereo representation of the ZnF UBP domain/ubiquitin complex. The ZnF UBP domain is colored in green, and ubiquitin is colored in gray. I44 and V70 of the hydrophobic patch of ubiquitin are shown in blue. L8 and I36 of ubiquitin (shown in magenta) interact with F224 of the ZnF UBP domain (shown in yellow).

ubiquitin in the chain occupy the same site. Thus, defects in the S1′ pocket are predicted to result in a decrease in polyubiquitin-chain hydrolysis. We tested whether one of the activation-defective IsoT point mutants (R221A) also exhibited a defect in the disassembly of K48-linked tetraubiquitin. As with ubiquitin-dependent modulation of Ub-AMC hydrolysis, R221A IsoT was also defective in the polyubiquitin-chain hydrolysis (Figures 5B–5C), indicating that the activation pocket or S1′ site has an important role in the disassembly of a physiological IsoT substrate.

Recognition of the C Terminus of Ubiquitin Is Conserved in the ZnF UBP Domain of scIMP

The ZnF UBP domain is a conserved domain present in other proteins of the ubiquitin system (Figure 4F). To test whether other ZnF UBP domains recognize ubiquitin by binding to its C terminus, we cloned and recombinantly expressed several ZnF UBP domains from other protein families. Only one of these expressed domains was soluble and was therefore purified for analysis, scIMP (YHL010c). scIMP is the *S. cerevisiae* homolog of human

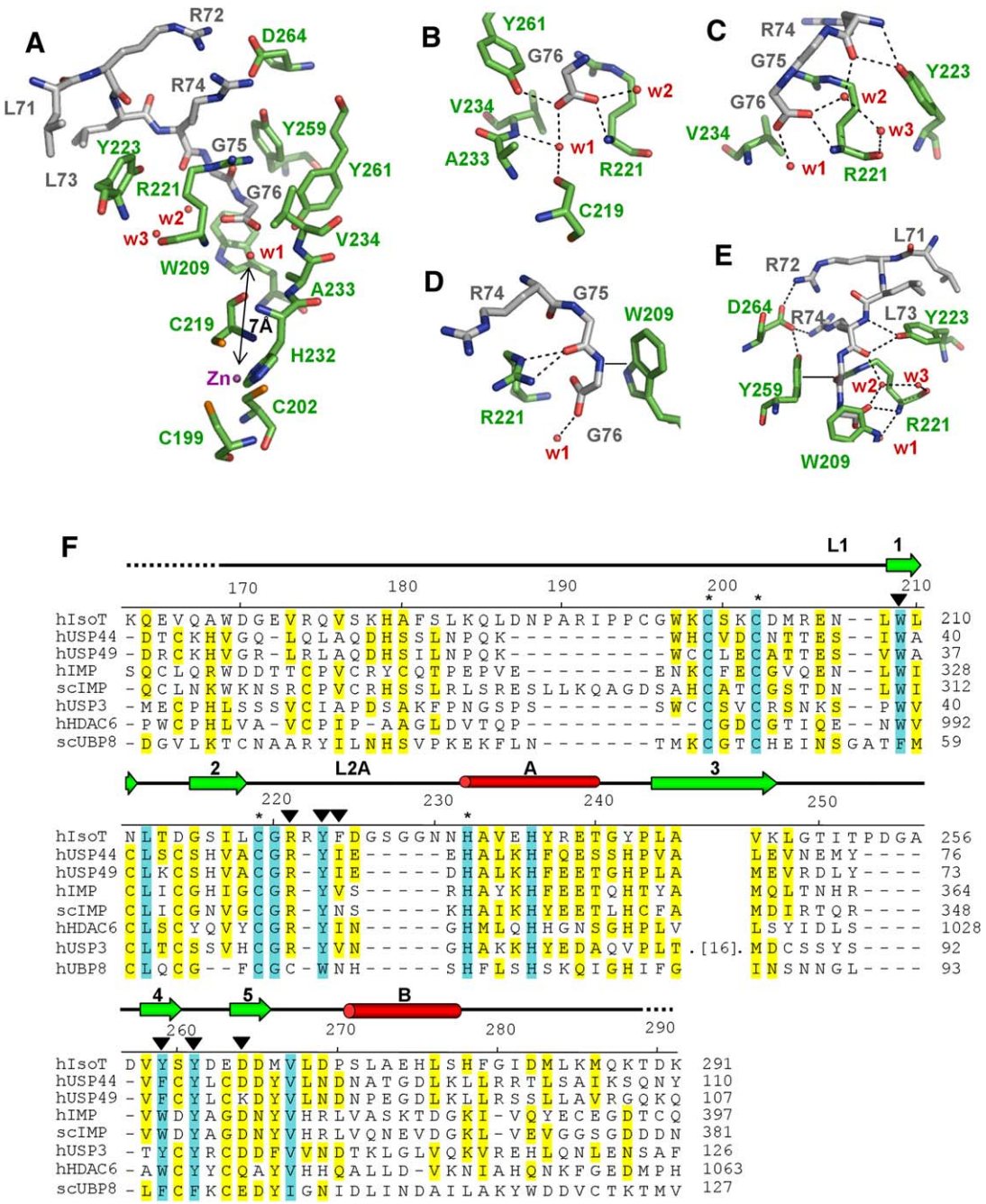

Figure 4. Interaction between Conserved Residues of the ZnF UBP Domain of IsoT and Ubiquitin

(A) Residues in the C terminus of ubiquitin (gray, carbons; dark blue, nitrogens; orange, sulfurs) interact with the Zn UBP domain (green, carbons; dark blue, nitrogens; orange, sulfurs). Water molecules and the Zn atom are shown as red spheres.

(B–E) Close-up of the interaction between the IsoT ZnF UBP domain and the C terminus of ubiquitin. Coloring is the same as above. Hydrogen bonds and electrostatic interactions are represented by black dashes.

(F) Sequence alignment of ZnF UBP domains. The sequence alignment was performed with ClustalW using the MegAlign software from DNAStar. The accession numbers from top to bottom are NP_003472, AAH30704, AAH14176, Q7Z569, AAS56441, AAH18113, NP_006035, and NP_013950. Secondary structure of the ZnF UBP domain of IsoT is shown above. Dashed lines indicate regions for which electron density was not observed. α helices are shown as cylinders and β sheets as arrows. The residues that chelate zinc are indicated by an asterisk. Residues that contact ubiquitin are indicated by triangles.

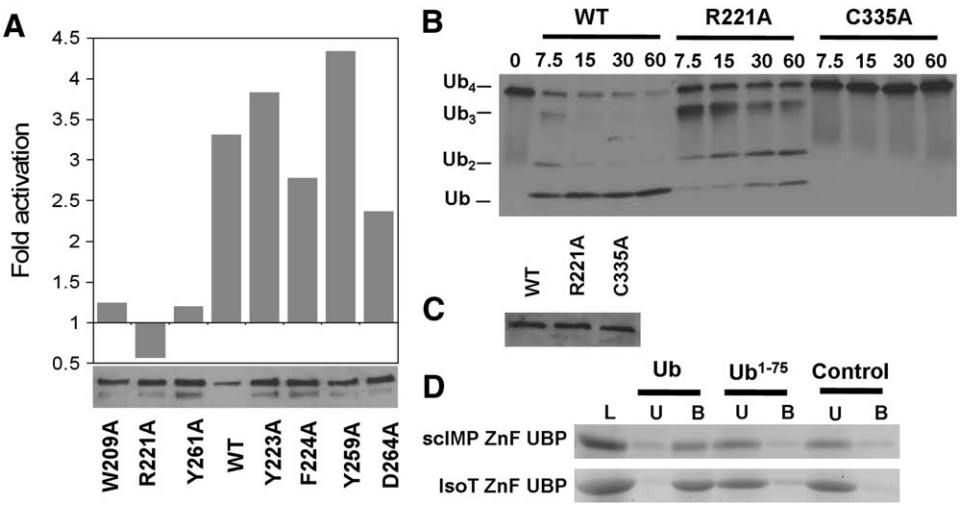

Figure 5. ZnF UBP Domain Residues Contacting the Diglycine Motif of Ubiquitin Are Required for Catalytic Activation of IsoT

(A) Effects of mutation of the residues contacting ubiquitin in the ZnF UBP domain of IsoT. *E. coli* cell lysates (8 ng/μl) expressing wild-type or ZnF UBP domain mutant IsoT were incubated with 48 nM Ub-AMC. After ~100 s, 177 nM Ub was added to the reaction. The fold activation was calculated by dividing the rate of the reaction after addition of ubiquitin by the rate before the addition of ubiquitin. A Western blot of *E. coli* cell lysate shows that equivalent amounts of wild-type or mutant IsoT were expressed (5 μg of cell lysate per lane).

(B) Hydrolysis of K48-linked tetraubiquitin (Ub_4) by wild-type, R221A, or C335A IsoT. Equivalent amounts of cell lysate (1.25 ng/μl) expressing WT, R221A, or C335A were incubated with excess of Ub_4 (10 ng/μl) for 7.5, 15, 30, and 60 min.

(C) Western blotting of the *E. coli* cell lysate expressing WT, R221A, and C335A IsoT (5 μg of cell lysate per lane) shows that equivalent amount of enzymes were added to the Ub_4 hydrolysis reaction shown in (B).

(D) The ZnF UBP domain of *S. cerevisiae* IMP (scIMP or YHL010c) binds ubiquitin and requires the C-terminal glycine of ubiquitin for binding. Purified IsoT or scIMP ZnF UBP domain was incubated with Ub, $Ub^{1–75}$, and control Sepharose beads. Load (L), unbound (U), and bound (B) ZnF UBP domain were analyzed by SDS-PAGE with SYPRO ruby staining.

IMP, sharing significant homology (34% identity) with the human protein, in particular within the ZnF UBP domain (65% identity). As shown in Figure 5D, the ZnF UBP domain of scIMP (residues 266–389) binds ubiquitin and, like the ZnF UBP domain of IsoT, fails to bind to $Ub^{1–75}$ or control resins. These results demonstrate that recognition of the C terminus of ubiquitin is conserved in another member of this domain family.

DISCUSSION

The Structure of the ZnF UBP Domain

The structure of the ZnF UBP domain is unique and does not closely resemble any other known structure. It has a compact globular fold with a deep cleft and a pocket that accommodates the C terminus of ubiquitin. A loop (L2A) forms a ruler that interacts with L8 and I36 on the face of ubiquitin but not with residues I44 or V70 (Figure 3B and Figure S1D), which are recognized by other ubiquitin binding domains (Hicke et al., 2005). Interactions between ubiquitin and the ZnF UBP domain are largely confined to this loop and to an extensive network of interactions between the walls of the ZnF UBP pocket and the C-terminal residues of ubiquitin. Three tyrosine residues and an arginine line the entrance to the pocket. It is likely that the initial interaction that results in threading the C terminus into the ZnF UBP pocket is an electrostatic interaction between this arginine (R221) and the negatively charged C terminus of unanchored polyubiquitin. This interaction must be followed by a further translocation of the ubiquitin such that the C terminus is inserted more deeply into the pocket as contacts are made between the binding surface of the cleft, as well as with the ruler loop (L2A) and the surface of ubiquitin containing L8 and I36. The extensive contacts with the diglycine motif of ubiquitin rationalizes IsoT's selectivity for an unmodified ubiquitin C terminus in binding and hydrolyzing unanchored polyubiquitin chains and explains the defect in chain disassembly observed in vivo when G76 is deleted (Amerik et al., 1997).

Residues Involved in Ubiquitin Binding Are Conserved in Other ZnF UBP Domains

The ZnF UBP domain is present in other proteins of the ubiquitin system (Figure 4F). These include the HDAC6 microtubule deacetylase; several mammalian deubiquitinating enzymes; and an E3 ligase, IMP (Amerik et al., 2000; Ingvarsdottir et al., 2005; Matheny et al., 2004; Quesada et al., 2004; Seigneurin-Berny et al., 2001). To date only the ZnF UBP domain of HDAC6 has been shown to bind ubiquitin (Hook et al., 2002; Seigneurin-Berny et al., 2001). The results of the present study indicate that two ZnF UBP domains, those of IsoT and scIMP, are also capable of binding ubiquitin, but not ubiquitin lacking its C-terminal glycine (Figure 5D).

The residues participating in ubiquitin recognition are conserved among other ZnF UBP domains (Figure 4F),

suggesting that the mode of binding may be similar in all cases. Most of the conserved residues (W209, R221, Y223, Y259, Y261, and D264) participate in recognition of the C terminus of ubiquitin by IsoT (Figure 4F). It is unclear what role this domain plays in other proteins; proteins that contain this domain might acts as sensors of ubiquitin or polyubiquitin levels, or they may participate in the conjugation of preformed polyubiquitin chains to target proteins. The latter role would be consistent with the presence of a RING finger ligase domain and a ZnF UBP domain in IMP. A preformed polyubiquitin chain could be bound by the ZnF UBP domain via its proximal end and positioned for the RING domain to catalyze conjugation by nucleophilic attack of a lysine of the target protein on the isopeptide linkage of the proximal ubiquitin. This simple transpeptidation would result in conjugation of the preformed chain less the proximal ubiquitin. Either mechanism could be involved in the observation that overexpression of UBP14 lowers steady-state levels of polyubiquitin and slows the degradation of some proteins in yeast (Amerik et al., 1997).

Role of the ZnF UBP Domain in Activation of Hydrolysis by IsoT

Our data show that the ZnF UBP domain contributes to the binding interactions that define the S1′ site of IsoT—that is, the site that binds the proximal ubiquitin in a polyubiquitin chain and that, upon binding monoubiquitin, activates the hydrolysis of ubiquitin-AMC bound in the S1 site (Dang et al., 1998; Stein et al., 1995). This activation is dependent upon the presence of an unmodified diglycine motif on the C terminus of ubiquitin, and our biochemical data demonstrate that these same requirements are evident in the binding of ubiquitin to the isolated ZnF UBP domain. Mutations in the ZnF UBP domain interfere with the activation of hydrolysis catalyzed by IsoT. The IsoT point mutants defective in activation also display a slight decrease in the rate of basal Ub-AMC hydrolysis. If the ZnF-UBP domain and catalytic domain have to interact for optimal activity, the mutations introduced may disturb that interaction equilibrium. Alternatively, this difference in the basal activity between the wild-type and the mutants may be due to activation of wild-type enzyme by the low levels of ubiquitin produced early in the hydrolysis of Ub-AMC. It is unlikely that the UBA domains (S2 and S3) of IsoT are responsible for activation of IsoT; several structural studies have conclusively shown that UBA domains bind to the I44 hydrophobic patch on ubiquitin and not to its C terminus (Mueller et al., 2004; Ohno et al., 2005; Varadan et al., 2005). Although our data do not rule out the possibility that the UBA domains work in conjunction with the ZnF UBP domain for activation of Ub-AMC hydrolysis, they do demonstrate that the ZnF UBP domain is indispensable for this activation.

The conformational change caused by binding of ubiquitin to the S1′ site provides a "proofreading" function that would assure that unanchored chains do not accumulate but would prevent IsoT from acting on chains until the conjugated protein/peptide has been removed by other deubiquitinating enzymes. To understand the nature of the conformational change that results in activation, we have compared the structure of the free and liganded domain. The only major difference between the structure of the ZnF UBP domain and the domain with ubiquitin bound is the orientation of the N terminus of the domain, although there is ~3.7 Å displacement of loop L2A to accommodate ubiquitin (Figure S3).The ZnF UBP domain crystallizes as a dimer linked by a disulfide bond between the C195 residues of both molecules (Figure S4A). The only significant contact between the two molecules is mediated through this disulfide bond. The ZnF UBP domain/ubiquitin complex also crystallized as a disulfide-linked dimer, but, unlike the unliganded domain, it has many intermolecular contacts formed by a 180° rotation of one monomer with respect to the other and a domain swap involving the N-terminal residues 173 to 196 (Figure S4B). Although in both structures the domain crystallized as a dimer, the dimerization was not observed in solution (data not shown), and there is no evidence that the full-length IsoT exists as a dimer. The significance of the IsoT ZnF UBP domain swapping is currently unknown; however, the alternative conformations of the N terminus may suggest that this region is flexible and thus could have a role in the putative conformational change that occurs upon activation of Ub-AMC hydrolysis.

Role of the ZnF UBP Domain in Polyubiquitin Recognition

IsoT can hydrolyze several different types of polyubiquitin chains (Raasi et al., 2005). Given that different types of polyubiquitin chains appear to have different conformations (Cook et al., 1994; Phillips et al., 2001; Varadan et al., 2002, 2004), it remains to be determined how IsoT can bind and hydrolyze all of them. One explanation is that the alternatively linked chains are flexible enough to adopt multiple conformations that can be accommodated by ubiquitin binding domains on IsoT. Another (not mutually exclusive) explanation is that IsoT has flexible linker regions that connect its different ubiquitin binding domains, and this flexibility allows the domains to be alternatively positioned so that they can accommodate each of the alternatively linked polyubiquitin chains. Kinetic and structural data on IsoT, combined with data on the flexibility of polyubiquitin chains, suggest that both the enzyme and the substrate may adapt (Phillips et al., 2001; Stein et al., 1995; Varadan et al., 2002, 2004).

A highly speculative model for this adaptation arises from the current structural data on ubiquitin binding to the ZnF UBP domain. The proximal ubiquitin in the chain is immobilized at S1′ by insertion of the C terminus deeply into a pocket in the ZnF UBP domain. The lysine residues involved in linking the next ubiquitin in a polyubiquitin chain do not contact the ZnF UBP domain, and thus the chain could project in any direction from the proximal ubiquitin, depending on the identity of the linkage. To hydrolyze different polyubiquitin chains, the relative orientation of the

ZnF UBP (S1′) and the UBP catalytic site (S1) would have to dramatically change, or the orientation of the bound proximal ubiquitin would have to vary in order to position the scissile bond near the catalytic site. We note that it is possible for the C terminus of the proximal ubiquitin to rotate like a ratchet in order to accommodate this alternative binding mode. Since the only significant contacts between the ZnF UBP domain and the body of ubiquitin are formed by interaction of the ruler loop L2A and the hydrophobic residues L8 and I36, rotation of the proximal ubiquitin about the R72 Ψ bond of the C terminus could position the proximal ubiquitin so that the ruler loop interacts instead with I44 and V70. This would allow the positioning of the scissile bond of alternatively linked polyubiquitin chains near the catalytic site without requiring so dramatic a change in the relative orientation of the S1 and S1′ sites. This model is currently being tested.

EXPERIMENTAL PROCEDURES

Fluorescence Anisotropy Measurements

Expression and purification of wild-type and mutant ubiquitins used in this study have been previously described (Yin et al., 2000). Ubiquitin bearing the K48C mutation was labeled for fluorescence anisotropy measurements with the thiol-selective fluorescent dye IAEDANS (5-((((2-iodoacetyl)amino)ethyl)amino)-naphthalene-1-sulfonic acid) (Molecular Probes, Inc). Labeling was carried out by reacting 14 μM K48C ubiquitin in 50 mM Tris (pH 7.5) buffer with 1.5 mM IAEDANS. The labeling reaction was incubated at 4°C for 24 hr in the dark followed by quenching by addition of 29 mM 2-mercaptoethanol. To remove the excess dye, the reaction was dialyzed extensively against 50 mM Tris (pH 7.5). About 95% of K48C ubiquitin was labeled with IAEDANS to give IA-Ub as determined by HPLC. Fluorescence anisotropy measurements were performed on an AMICO-BOWMAN Series 2 Luminescence Spectrometer at 37°C. A constant amount of IA-Ub (80 nM) was incubated with or without wild-type ubiquitin or $Ub^{1–75}$, and increasing amounts of wild-type or C199A IsoT were added to the mixture. Wild-type and C199A IsoT concentrations were determined using an ε_{280} of 86,290 $cm^{-1}M^{-1}$ (Gill and von Hipple, 1989). Binding constants were calculated as described previously (Wilkinson, 2004) using Origin 7.0 software (OriginLab Corporation).

Limited Proteolysis of Full-Length IsoT

Full-length IsoT was expressed in *E. coli* and purified as previously described (Russell and Wilkinson, 2005). To determine the borders of the ZnF UBP domain, we performed limited proteolysis on the full-length protein. IsoT was incubated with 1:10 (w/w) trypsin in 50 mM Tris, 1 mM $CaCl_2$, 2 mM 2-mercaptoethanol (pH 8.0). The reaction was incubated at 4°C for 30 min and then quenched by inactivating trypsin with PMSF (10 μM final concentration). NaCl and Triton X-100 were added to the reaction to a final concentration of 150 mM and 10% (v/v), respectively. To select for a fragment that binds ubiquitin with an intact C terminus, 40 μg of digested IsoT was incubated with 100 μl of monoubiquitin, G76C monoubiquitin, or control Sepharose resins for 3 hr at 4°C. The resins were synthesized by incubating the ligands with Sepharose 4B resins preactivated with divinyl sulfone (Hermanson et al., 1992). After blocking with glycine ethyl ester, the resins contained 8 mg/ml immobilized protein. After applying the tryptic digest, the resins were washed three times with 100 μl 50 mM Tris, 2 mM DTT, 150 mM NaCl (pH 7.3). Fragments of IsoT that bound to the resins were eluted by boiling in 1× SDS loading buffer. The bound and unbound fractions were analyzed by SDS-PAGE. A 15 kDa fragment that bound the ubiquitin Sepharose resin, but not the G76C or control resins, was excised from the SDS-PAGE gel and analyzed by matrix-assisted laser desorption/ionization mass spectroscopy (MALDI-MS) and N-terminal sequencing (Microchemical Facility, Emory University).

Expression and Purification of the ZnF UBP Domains of IsoT and scIMP

The ZnF UBP domain of IsoT (163–291) was subcloned between the NdeI and HindIII sites of pRSET B (Invitrogen) using standard molecular biology methods. Expression was carried out as described for full-length IsoT. The ZnF UBP domain of IsoT was purified using a ubiquitin column similar to full-length IsoT (Gabriel et al., 2002; Russell and Wilkinson, 2005). The purified protein was chromatographed on a 160 ml gel filtration column (Sephacryl S-100 resin) equilibrated with 50 mM Tris, 150 mM NaCl, 2 mM β-mecaptoethanol (pH 7.5). Fractions containing the ZnF UBP domain were identified by SDS-PAGE, pooled, and concentrated. Protein concentration was measured using ε_{280} = 23,950 $cm^{-1}M^{-1}$ (Gill and von Hipple, 1989). The ZnF UBP domain of scIMP (266–389) was PCR amplified from yeast genomic DNA, and a His_6 tag was introduced at the 5′ end of the coding sequence. The amplified DNA was subcloned between the NdeI and HindIII sites of pRSET B. Expression was carried out as described for the full-length IsoT, and the protein was purified using Ni-NTA agarose resin (QIAGEN).

Isothermal Titration Calorimetry

The ZnF UBP domain of IsoT and ubiquitin were dialyzed extensively against 50 mM Tris-HCl buffer, 150 mM NaCl, 2 mM β-mercaptoethanol (pH 7.5). ITC measurements were carried out in triplicate on a MicroCal VP-ITC instrument at 30°C. Ubiquitin (1362 μM) was injected into 1.4 ml of buffer containing ZnF UBP domain (50 μM) in 35 injections of 3 μl each. Binding constants were calculated by fitting the data using Origin 7.0 (OriginLab Corporation).

Site-Directed Mutagenesis of the ZnF UBP Domain of Full-Length Isopeptidase T

Plasmid DNA encoding full-length IsoT (pRSIsoT) was mutagenized using the QuikChange Site-Directed Mutagenesis Kit (Stratagene, Inc). The point mutants were expressed in *E. coli* as described for wild-type IsoT. C199A IsoT was purified as described for the wild-type protein.

Ub-AMC Hydrolysis

Enzymatic activity was measured by incubation of Ub-AMC with *E. coli* cell lysate expressing wild-type or point mutant IsoT at 37°C in 50 mM Tris-HCl, 1 mM DTT, 10 μg/ml ovalbumin (pH 7.5). Immunoblots using rabbit anti-IsoT antibodies generated against the full-length recombinant protein showed that a similar level of expression is achieved in all cases. The reaction was monitored by following the increase in fluorescence at 440 nm (λ_{ex} = 340 nm). The activation of Ub-AMC hydrolysis by ubiquitin was measured by adding 85 or 117 nM of ubiquitin 100 s after adding IsoT to the Ub-AMC reaction mixture.

K48-Linked Tetraubiquitin Hydrolysis

We incubated 10 ng/μl of tetraubiquitin (Boston Biochem, Inc.) with or without lysates (1.25 ng/μl) containing recombinant wild-type, R221A, or C335A IsoT for varying times. The incubation was carried out at 37°C in 50 mM Tris (pH 8.0), 150 mM NaCl, 10 mM β-mercaptoethanol, and 0.5 μg/μl BSA. Samples were analyzed by SDS-PAGE and immunochemical analysis using antibodies to ubiquitin (clone P4D1; Santa Cruz Biotechnology, Inc.). Immunoblots of the cell lysate using IsoT antibodies showed that equivalent amounts of IsoT point mutants were added to each reaction.

Ubiquitin Resin Binding

We incubated 40 μg of purified IsoT or scIMP (YHL010c) ZnF UBP domain (100 μl of 50 mM Tris [pH 8.0], 150 mM NaCl, 10 mM β-mercaptoethanol, and 0.1% Triton X-100) with or without 50 μl of blocked

control, ubiquitin (8 mg/ml), or ubiquitin$^{1-75}$ (8 mg/ml) conjugated Sepharose resins, for 3 hr at 4°C. Equal ratios of bound and unbound fractions were analyzed by SDS-PAGE and SYPRO ruby staining (Molecular Probes, Inc).

Crystallography

The ZnF UBP domain of IsoT was concentrated to 32 mg/ml and crystallized by vapor diffusion (2 μl hanging drops over 1 ml reservoirs of 18% polyethylene glycol 8000, 0.1 M sodium cacodylate [pH 6.5], 0.2 M calcium acetate). Crystals (C2 space group) were cryoprotected in 16% polyethylene glycol 8000, 0.8 M sodium cacodylate (pH 6.5), 0.16 M calcium acetate, 20% glycerol and frozen in liquid nitrogen. The ZnF UBP domain/ubiquitin complex was prepared by incubating 2-fold molar excess of ubiquitin with the ZnF UBP domain. The complex was separated from unbound ubiquitin by gel filtration (Sephacryl S-100 resin). The complex was concentrated to 32 mg/ml. The ZnF UBP domain/ubiquitin complex was crystallized by vapor diffusion (2 μl hanging drops over 1 ml reservoirs of 16% polyethylene glycol 8000, 0.08 M sodium cacodylate [pH 6.5], 0.16 M magnesium or calcium acetate, and 20% ethylene glycol). The structure of the ZnF UBP domain was determined utilizing zinc multiwavelength anomalous dispersion (MAD) phasing (Table S1). Three datasets, at wavelengths of 1.1281, 1.2790, and 1.2802 Å, were required for the program SOLVE to find the positions of two zinc atoms (one for each molecule, two molecules per asymmetric unit) to give a solution with a high figure of merit (0.49 using 2.3 Å data cutoff). 176 out of 260 residues were built and 136 side chains were placed utilizing the RESOLVE iterative model-building script. The remaining residues were then built manually, first into the electron density map from the RESOLVE optimized phases and the partially refined models and then into densities of difference maps using the program O (Jones and Kjeldgaard, 1997) and refinement with the program CNS (Brunger et al., 1998). Refinement to a resolution of 2.09 Å was carried out with data collected at 0.97623 Å for another crystal. The structure of the complex of the ZnF UBP domain with ubiquitin was also solved with zinc MAD phasing using data collected at the Advanced Photon Source SER-CAT 22-ID beamline (Table S2). The program REPLACE (Tong and Rossmann, 1997) located the position of the ZnF UBP domain by molecular replacement but could not locate the ubiquitin molecule. The program SOLVE was used with four wavelength data sets (1.27163, 1.28237, 1.28317, and 1.28855 Å), and RESOLVE iterative model-building script automatically built most of the ubiquitin molecule and some of ZnF UBP domain in the complex. A model of the complex was built for refinement by least-squares fitting of the partially built structure with the previously determined ZnF UBP domain and a known ubiquitin structure (PDB ID code 1UBQ) except for a substitution of the C terminus of ubiquitin with that built by RESOLVE. Refinement to a resolution of 1.99 Å was carried out with data collected at 1.0000 Å for another crystal and proceeded by examination of difference electron densities. In both structures, there are two molecules/complexes per asymmetric unit. Drawings were produced using PyMOL, USCF Chimera (Pettersen et al., 2004), and GRASP (Nicholls et al., 1991).

Supplemental Data

Supplemental Data include four figures and two tables and can be found with this article online at http://www.cell.com/cgi/content/full/124/6/1197/DC1/.

ACKNOWLEDGMENTS

We thank Linda Hicke for the GST-Ub and GST-Ub I44A constructs and Francesco Melandri for the K48-linked tetraubiquitin. X-ray data collection for the ZnF UBP domain were collected at the beamline X26C of National Synchrotron Light Source, Brookhaven National Laboratory. X-ray data for the complex were collected at beamline 22-ID in the facilities of SER-CAT at the Advanced Photon Source, Argonne National Laboratory. Use of the Advanced Photon Source was supported by the US Department of Energy, Office of Science, Office of Basic Energy Sciences under Contract No. W-31-109-Eng-38. This work is supported in part by NIH training grants 5T32GM008367 and 1F31GM075426-01 to F.E.R.-T., NIH grant GM30308 to K.D.W., and NIH grant GM068680 to J.R.H. and X.C.

Received: September 30, 2005
Revised: January 14, 2006
Accepted: February 28, 2006
Published: March 23, 2006

REFERENCES

Alam, S.L., Sun, J., Payne, M., Welch, B.D., Blake, B.K., Davis, D.R., Meyer, H.H., Emr, S.D., and Sundquist, W.I. (2004). Ubiquitin interactions of NZF zinc fingers. EMBO J. *23*, 1411–1421.

Amerik, A., Swaminathan, S., Krantz, B.A., Wilkinson, K.D., and Hochstrasser, M. (1997). In vivo disassembly of free polyubiquitin chains by yeast Ubp14 modulates rates of protein degradation by the proteasome. EMBO J. *16*, 4826–4838.

Amerik, A.Y., and Hochstrasser, M. (2004). Mechanism and function of deubiquitinating enzymes. Biochim. Biophys. Acta *1695*, 189–207.

Amerik, A.Y., Li, S.J., and Hochstrasser, M. (2000). Analysis of the deubiquitinating enzymes of the yeast Saccharomyces cerevisiae. Biol. Chem. *381*, 981–992.

Bienko, M., Green, C.M., Crosetto, N., Rudolf, F., Zapart, G., Coull, B., Kannouche, P., Wider, G., Peter, M., Lehmann, A.R., et al. (2005). Ubiquitin-binding domains in Y-family polymerases regulate translesion synthesis. Science *310*, 1821–1824.

Brunger, A.T., Adams, P.D., Clore, G.M., DeLano, W.L., Gros, P., Grosse-Kunstleve, R.W., Jiang, J.S., Kuszewski, J., Nilges, M., Pannu, N.S., et al. (1998). Crystallography & NMR system: A new software suite for macromolecular structure determination. Acta Crystallogr. D Biol. Crystallogr. *54*, 905–921.

Cook, W.J., Jeffrey, L.C., Kasperek, E., and Pickart, C.M. (1994). Structure of tetraubiquitin shows how multiubiquitin chains can be formed. J. Mol. Biol. *236*, 601–609.

Dang, L.C., Melandri, F.D., and Stein, R.L. (1998). Kinetic and mechanistic studies on the hydrolysis of ubiquitin C-terminal 7-amido-4-methylcoumarin by deubiquitinating enzymes. Biochemistry *37*, 1868–1879.

Davies, B.A., Topp, J.D., Sfeir, A.J., Katzmann, D.J., Carney, D.S., Tall, G.G., Friedberg, A.S., Deng, L., Chen, Z., and Horazdovsky, B.F. (2003). Vps9p CUE domain ubiquitin binding is required for efficient endocytic protein traffic. J. Biol. Chem. *278*, 19826–19833.

Doelling, J.H., Yan, N., Kurepa, J., Walker, J., and Vierstra, R.D. (2001). The ubiquitin-specific protease UBP14 is essential for early embryo development in Arabidopsis thaliana. Plant J. *27*, 393–405.

Gabriel, J.M., Lacombe, T., Carobbio, S., Paquet, N., Bisig, R., Cox, J.A., and Jaton, J.C. (2002). Zinc is required for the catalytic activity of the human deubiquitinating isopeptidase T. Biochemistry *41*, 13755–13766.

Gill, S.C., and von Hipple, P.H. (1989). Calculation of protein extinction coefficients from amino acid sequence data. Anal. Biochem. *182*, 319–326.

Hermanson, G.T., Krishna, A., and Smith, P.K. (1992). Activation methods. In Immobilized Affinity Ligand Techniques (San Diego, CA: Academic Press, Inc.), pp. 80–90.

Hershko, A., and Ciechanover, A. (1998). The ubiquitin system. Annu. Rev. Biochem. *67*, 425–479.

Hicke, L. (2001). Protein regulation by monoubiquitin. Nat. Rev. Mol. Cell Biol. *2*, 195–201.

Hicke, L., Schubert, H.L., and Hill, C.P. (2005). Ubiquitin-binding domains. Nat. Rev. Mol. Cell Biol. *6*, 610–621.

Hook, S.S., Orian, A., Cowley, S.M., and Eisenman, R.N. (2002). Histone deacetylase 6 binds polyubiquitin through its zinc finger (PAZ domain) and copurifies with deubiquitinating enzymes. Proc. Natl. Acad. Sci. USA *99*, 13425–13430.

Ingvarsdottir, K., Krogan, N.J., Emre, N.C., Wyce, A., Thompson, N.J., Emili, A., Hughes, T.R., Greenblatt, J.F., and Berger, S.L. (2005). H2B ubiquitin protease Ubp8 and Sgf11 constitute a discrete functional module within the Saccharomyces cerevisiae SAGA complex. Mol. Cell. Biol. *25*, 1162–1172.

Jones, T.A., and Kjeldgaard, M. (1997). Electron-density map interpretation. Methods Enzymol. *277*, 173–208.

Lam, Y.A., Pickart, C.M., Alban, A., Landon, M., Jamieson, C., Ramage, R., Mayer, R.J., and Layfield, R. (2000). Inhibition of the ubiquitin-proteasome system in Alzheimer's disease. Proc. Natl. Acad. Sci. USA *97*, 9902–9906.

Lee, S., Tsai, Y.C., Mattera, R., Smith, W.J., Kostelansky, M.S., Weissman, A.M., Bonifacino, J.S., and Hurley, J.H. (2006). Structural basis for ubiquitin recognition and autoubiquitination by Rabex-5. Nat. Struct. Mol. Biol., in press. Published online February 5, 2006. 10.1038/nsmb1064.

Li, S., Ku, C.Y., Farmer, A.A., Cong, Y.S., Chen, C.F., and Lee, W.H. (1998). Identification of a novel cytoplasmic protein that specifically binds to nuclear localization signal motifs. J. Biol. Chem. *273*, 6183–6189.

Lindsey, D.F., Amerik, A., Deery, W.J., Bishop, J.D., Hochstrasser, M., and Gomer, R.H. (1998). A deubiquitinating enzyme that disassembles free polyubiquitin chains is required for development but not growth in Dictyostelium. J. Biol. Chem. *273*, 29178–29187.

Matheny, S.A., Chen, C., Kortum, R.L., Razidlo, G.L., Lewis, R.E., and White, M.A. (2004). Ras regulates assembly of mitogenic signalling complexes through the effector protein IMP. Nature *427*, 256–260.

Mueller, T.D., Kamionka, M., and Feigon, J. (2004). Specificity of the interaction between ubiquitin-associated domains and ubiquitin. J. Biol. Chem. *279*, 11926–11936.

Nicholls, A., Sharp, K.A., and Honig, B. (1991). Protein folding and association: insights from the interfacial and thermodynamic properties of hydrocarbons. Proteins *11*, 281–296.

Ohno, A., Jee, J., Fujiwara, K., Tenno, T., Goda, N., Tochio, H., Kobayashi, H., Hiroaki, H., and Shirakawa, M. (2005). Structure of the UBA domain of Dsk2p in complex with ubiquitin: molecular determinants for ubiquitin recognition. Structure (Camb.) *13*, 521–532.

Penengo, L., Mapelli, M., Murachelli, A.G., Confalonieri, S., Magri, L., Musacchio, A., Di Fiore, P.P., Polo, S., and Schneider, T.R. (2006). Crystal structure of the ubiquitin binding domains of Rabex-5 reveals two modes of interaction with ubiquitin. Cell *124*, this issue, 1183–1195. Published online February 16, 2006. 10.1016/jcell200602020.

Pettersen, E.F., Goddard, T.D., Huang, C.C., Couch, G.S., Greenblatt, D.M., Meng, E.C., and Ferrin, T.E. (2004). UCSF Chimera—a visualization system for exploratory research and analysis. J. Comput. Chem. *25*, 1605–1612.

Phillips, C.L., Thrower, J., Pickart, C.M., and Hill, C.P. (2001). Structure of a new crystal form of tetraubiquitin. Acta Crystallogr. D Biol. Crystallogr. *57*, 341–344.

Pickart, C.M. (2004). Back to the future with ubiquitin. Cell *116*, 181–190.

Pickart, C.M., and Fushman, D. (2004). Polyubiquitin chains: polymeric protein signals. Curr. Opin. Chem. Biol. *8*, 610–616.

Prag, G., Misra, S., Jones, E.A., Ghirlando, R., Davies, B.A., Horazdovsky, B.F., and Hurley, J.H. (2003). Mechanism of ubiquitin recognition by the CUE domain of Vps9p. Cell *113*, 609–620.

Prag, G., Lee, S., Mattera, R., Arighi, C.N., Beach, B.M., Bonifacino, J.S., and Hurley, J.H. (2005). Structural mechanism for ubiquitinated-cargo recognition by the Golgi-localized, gamma-ear-containing, ADP-ribosylation-factor-binding proteins. Proc. Natl. Acad. Sci. USA *102*, 2334–2339.

Quesada, V., Diaz-Perales, A., Gutierrez-Fernandez, A., Garabaya, C., Cal, S., and Lopez-Otin, C. (2004). Cloning and enzymatic analysis of 22 novel human ubiquitin-specific proteases. Biochem. Biophys. Res. Commun. *314*, 54–62.

Raasi, S., Varadan, R., Fushman, D., and Pickart, C.M. (2005). Diverse polyubiquitin interaction properties of ubiquitin-associated domains. Nat. Struct. Mol. Biol. *12*, 708–714.

Russell, N.S., and Wilkinson, K.D. (2005). Deubiquitinating enzyme purification, assay inhibitors, and characterization. Methods Mol. Biol. *301*, 207–219.

Seigneurin-Berny, D., Verdel, A., Curtet, S., Lemercier, C., Garin, J., Rousseaux, S., and Khochbin, S. (2001). Identification of components of the murine histone deacetylase 6 complex: link between acetylation and ubiquitination signaling pathways. Mol. Cell. Biol. *21*, 8035–8044.

Sigismund, S., Polo, S., and Di Fiore, P.P. (2004). Signaling through monoubiquitination. Curr. Top. Microbiol. Immunol. *286*, 149–185.

Stein, R.L., Chen, Z., and Melandri, F. (1995). Kinetic studies of isopeptidase T: modulation of peptidase activity by ubiquitin. Biochemistry *34*, 12616–12623.

Sun, L., and Chen, Z.J. (2004). The novel functions of ubiquitination in signaling. Curr. Opin. Cell Biol. *16*, 119–126.

Sundquist, W.I., Schubert, H.L., Kelly, B.N., Hill, G.C., Holton, J.M., and Hill, C.P. (2004). Ubiquitin recognition by the human TSG101 protein. Mol. Cell *13*, 783–789.

Swanson, K.A., Kang, R.S., Stamenova, S.D., Hicke, L., and Radhakrishnan, I. (2003). Solution structure of Vps27 UIM-ubiquitin complex important for endosomal sorting and receptor downregulation. EMBO J. *22*, 4597–4606.

Tong, L., and Rossmann, M.G. (1997). Rotation function calculations with GLRF program. Methods Enzymol. *276*, 594–611.

Varadan, R., Walker, O., Pickart, C., and Fushman, D. (2002). Structural properties of polyubiquitin chains in solution. J. Mol. Biol. *324*, 637–647.

Varadan, R., Assfalg, M., Haririnia, A., Raasi, S., Pickart, C., and Fushman, D. (2004). Solution conformation of Lys63-linked di-ubiquitin chain provides clues to functional diversity of polyubiquitin signaling. J. Biol. Chem. *279*, 7055–7063.

Varadan, R., Assfalg, M., Raasi, S., Pickart, C., and Fushman, D. (2005). Structural determinants for selective recognition of a Lys48-linked polyubiquitin chain by a UBA domain. Mol. Cell *18*, 687–698.

Welchman, R.L., Gordon, C., and Mayer, R.J. (2005). Ubiquitin and ubiquitin-like proteins as multifunctional signals. Nat. Rev. Mol. Cell Biol. *6*, 599–609.

Wilkinson, K.D. (1997). Regulation of ubiquitin-dependent processes by deubiquitinating enzymes. FASEB J. *11*, 1245–1256.

Wilkinson, K.D. (2004). Quantitative analysis of protein-protein interactions. Methods Mol. Biol. *261*, 15–32.

Wilkinson, K.D., Tashayev, V.L., O'Connor, L.B., Larsen, C.N., Kasperek, E., and Pickart, C.M. (1995). Metabolism of the polyubiquitin degradation signal: structure, mechanism, and role of isopeptidase T. Biochemistry *34*, 14535–14546.

Yin, L., Krantz, B., Russell, N.S., Deshpande, S., and Wilkinson, K.D. (2000). Nonhydrolyzable diubiquitin analogues are inhibitors of ubiquitin conjugation and deconjugation. Biochemistry *39*, 10001–10010.

Accession Numbers

The crystallographic coordinates for IsoT ZnF and IsoT-ubiquitin have been deposited in the Protein Data Bank with the ID codes 2G43 and 2G45, respectively.